3D Activity Recognition using Motion History and Binary Shape Templates

Saumya Jetley

Fabio Cuzzolin

Oxford Brookes University

Abstract.

This paper presents our work on activity recognition in 3D depth images. We propose a global descriptor that is accurate, compact and easy to compute as compared to the state-of-the-art for characterizing depth sequences. Activity enactment video is divided into temporally overlapping blocks. Each block (set of image frames) is used to generate Motion History Templates (MHTs) and Binary Shape Templates (BSTs) over three different views - front, side and top. The three views are obtained by projecting each video frame onto three mutually orthogonal Cartesian planes. MHTs are assembled by stacking the difference of consecutive frame projections in a weighted manner separately for each view. Histograms of oriented gradients are computed and concatenated to represent the motion content. Shape information is obtained through a similar gradient analysis over BSTs. These templates are built by overlaying all the body silhouettes in a block, separately for each view. To effectively trace shape-growth, BSTs are built additively along the blocks.

Consequently, the complete ensemble of gradient features carries both 3D shape and motion information to effectively model the dynamics of an articulated body movement. Experimental results on 4 standard depth databases (MSR 3D Hand Gesture, MSR Action, Action-Pairs, and UT-Kinect) prove the efficacy as well as the generality of our compact descriptor. Further, we successfully demonstrate the robustness of our approach to (impulsive) noise and occlusion errors that commonly affect depth data.

Keywords: video sequence, action recognition, depth sequence, depth image, temporal block

1. Introduction.

Action recognition from video sequences is a widely explored challenge, which continues to be the subject of active research. With important applications in the areas of video surveillance, video indexing/retrieval, human-computer interaction (in particular for gaming consoles or surgical assistance), robotic navigation and many others, the task of human activity recognition has immense practical value. Research in this field began on RGB video sequences captured by single traditional cameras – proven successful approaches to static image analysis were extrapolated to cater to the additional time axis. Such techniques can be typically categorized into local descriptor [1], [2], [3] and global descriptor-based [4], [5], [6] approaches.

More recently, the advent of affordable depth cameras has shifted the focus onto depth images, which can now be easily recorded in real-time with good accuracies. Besides providing clear advantages in terms of illumination invariance and robust foreground extraction, range images also encode shape and motion information which (if represented efficiently) can facilitate much improved activity recognition results.

Depth images, however, need to be treated differently from their colored counterparts. Any attempt to use local differential operators tends to fail, due to false firing on discontinuous black regions of undefined depth values. As confirmed in [7], for MSR Daily Activity Dataset [8] 60% of the identified Dollar interest points [2] were empirically observed at locations irrelevant to the action . Thus, interest-point based 2D video analysis approaches like STIP [1] have been shown inadequate to deal with 3D depth data.

The development of robust approaches to the quick and accurate estimation of 3D joint positions of human body from a single depth image [9] have spurred substantial research work, aimed at achieving action recognition through skeleton tracking [8,10,11,12]. [8], for instance, proposes the use of Fourier pyramids to represent the temporal dynamics of 3D joint-positions, learned using discriminative actionlet pools and a multiple kernel based approach. Li Xia et al. [13] also employ 3D skeletal joint positions for action recognition. Although these approaches do yield good practical accuracies, 3D joint positions are prone to noise and even partial occlusion can drastically affect recognition. Also, until recently, due to the difficulty of efficient skeleton tracking for hands these approaches were not employable in hand gesture recognition. Although the approach in [14] has overcome such a limitation, the additional tracking step is still susceptible to occlusion problems.

Approaches which do not make use of skeleton tracking have been proposed. In [15] an 'action graph' based on bag of 3D contour points is used to identify action classes. Methods based on dense sampling have also been attempted, which perform a grid-based analysis of the 4D spatio-temporal volume [7] associated with a depth sequence for recognizing actions [16]. Although such methods can be improved by introducing random sampling of sub-volumes [17] to reduce computation cost and make the features more discriminative, they are still computationally demanding, both during training and testing.

Bobick & Davis [18] introduced the concepts of Motion Energy Templates (METs) and Motion History Templates (MHTs) in traditional videos. They recognized body movements in input RGB sequences using Hu-moments based statistical models built from above templates. Subsequently, Davis [19] improved on the approach by using an MHT pyramid to account for varying action-enactment speeds, and characterized the resulting motion field using a polar histogram. Tian et al. [20] also employed MHTs for action recognition in crowded scene videos, owing to its effectiveness in capturing continuous and recent foreground motion even in a cluttered and inconsistently moving background. Using Harris corner points to eliminate noisy motion from MHT, they computed gradient features from intensity image and MHT. The features were learnt by a Gaussian Mix-ture Model (GMM) based classifier. However, it was Yang et al. [21] who first extended the idea to 3D depth images. They adopted METs and stacked motion regions for entire video sequences over three distinct views – front, side and top. Gradient features for the 3 consolidated binary templates were then used to represent depth sequences.

1.1 Contribution.

Based on the conducted critical review of past approaches and their limitations we propose a highly discriminative ensemble of both shape and motion features, extracted over a novel temporal construct formed by overlapping video blocks, for 3D action recognition from depth sequences.

First of all, contrarily to [21] where a single template is built over the complete video sequence, we build and analyze motion and shape templates separately for overlapping temporal blocks. The intuition behind this novel temporal construct and its discriminative advantages are elaborated in

3.1. By dividing the video sequence in smaller temporal blocks, we prevent the loss of motion information which happens when a more recent action overwrites an old action at the same point. Temporal overlap across blocks maintains continuity in the templates.

Secondly, instead of using Depth Motion Maps (a form of METs) as in [21], we adopt Motion History Templates so as to effectively capture information on the direction of motion, in the form of gray level variations. This allows our approach to cope successfully with sequences like those in the 3D Action Pairs database [7], in which the direction of motion is the essential discriminating factor.

In an additional original feature of our proposal, METs are assembled over temporal blocks in an accumulative manner to capture shape information. The shape of the resulting black and white boundaries describes how the human body envelope grows in the course of a certain action.

Finally, histograms of oriented gradients extracted from these templates are concatenated to yield the final feature vector. The latter constitutes a novel, low-dimensional, computationally inexpensive and highly discriminative global descriptor for depth sequences. This descriptor is used to train a non-linear large-margin classifier (RBF kernel based SVM) to identify action classes. The complete process flow is shown in Fig.1.

The generality of the approach is empirically demonstrated by evaluating it on 4 standard depth benchmarks – the 3D Hand Gesture, 3D Action, Action Pair, and UT-Kinect datasets. A vanilla implementation of our method outperforms the existing-best on 2 out of three 3 standard benchmarks, and has performance equal to the state of the art on the skeleton-biased UT-Kinect dataset. Note that our approach uses a block-size and an overlap-factor as parameters, that are in these experiments still manually selected by trial & error. By setting these parameters via cross validation our work has much scope for further performance gains.

Last but not least, in tests commonly neglected in the literature, we experimentally demonstrate the robustness of our approach to noise and occlusions that typically affect depth images by artificially corrupting sequences from the MSR 3D Action dataset. Results show that performance is remarkably robust to both nuisances, making our approach suitable for real-world deployment.

1.2 Paper outline.

The paper is organized as follows. Section 2 compares our approach in detail with the closest related work. Section 3 illustrates the various steps of the proposed approach. Section 4 recalls the benchmark datasets considered in our tests and details the experimental settings. The performance of our algorithm on the four considered benchmarks is illustrated in Section 5. Section 6 studies the robustness of the approach against common occlusion and noise errors. Section 7 concludes the paper with a word about the future directions of research.
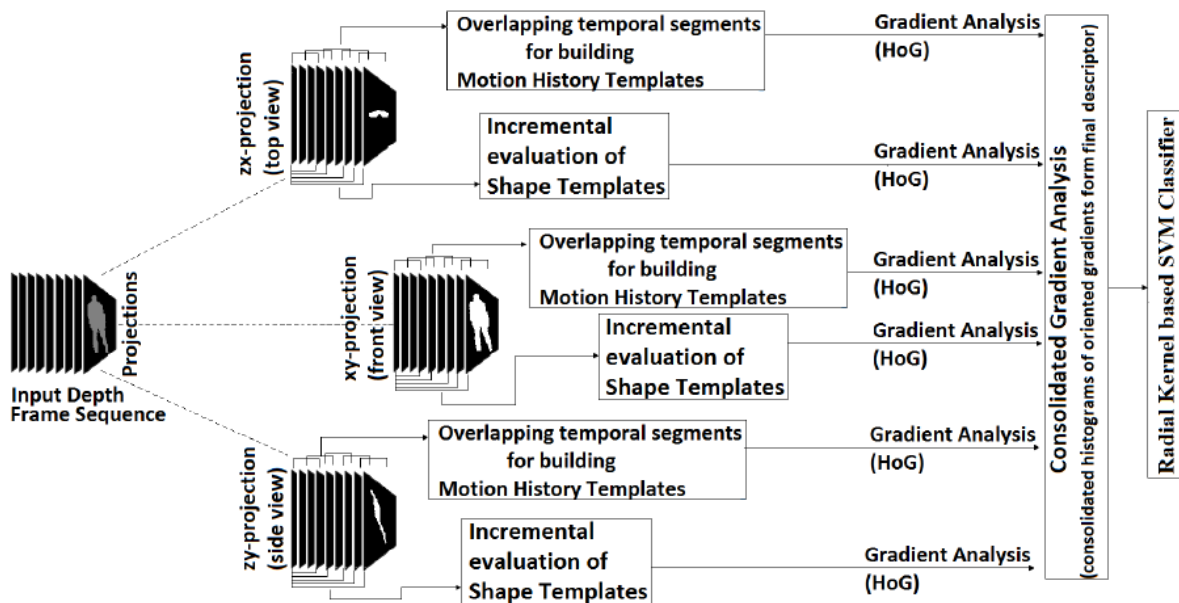
Fig. 1: Process flow for the proposed 3D activity recognition approach.

2. Relevant Related Work.

Vennila et al.[22] follow a similar idea to that proposed in our approach, but in a rather more simplistic way. Motion and 3D shape information are not considered in conjunction. Their analysis of only frontal MHIs leaves out depth (3D shape) information, while their Average Depth and Difference Depth Images do not consider motion and thus capture background-clutter depth details also.

Weinland et al. [23] suggest the use of motion history volumes for analyzing voxelset sequences. Their normalization along the r & z axes may cause alignment failure, like confusion between a person spreading his arms and a person dropping them. The Fourier analysis that they apply in concentric circles at each height does not capture limb movement as well as our gradient analysis of MHTs. For composite actions such as the walking gait, only one temporal segment is used. All these cause confusion between well distinct actions such as sit-down & pick-up, turn-around & majority-of-other-actions, walk & pick-up or kick. Also, the used 1D-FT overlooks motion symmetry around z axis and may fail to distinguish between single & two arm waves, forward & side punch, and forward & side kick.

Finally, Oreifej and Liu [7] represent the current state-of-the-art for the task at hand. Their method computes and concatenates the histograms of oriented surface normals for each grid cell and uses the final feature descriptor to train an SVM classifier. We compare ourselves to [7] empirically in Section 5.

3. Proposed Approach.

 In a depth image, each pixel contains a value which is a function of the depth/distance at which the camera encounters an object at the corresponding point in the real scene. For a depth camera recording from the front, the information of overlapped object points in the rear is not captured. Therefore, a depth image at any time does not contain an exact all-view model of the 3D objects present in the scene. Nonetheless, the data is sufficient to generate three approximate front, side and top views of the scene which, for a single 3D object, contain important, non-redundant and discriminative information both in terms of shape (over a single frame) and motion (over a sequence of frames). It is to obtain and leverage this enhanced 3D shape and motion information that we first project each frame of the incoming video sequence onto the three orthogonal Cartesian planes. The front, side and top views so obtained for a given frame are as illustrated in Fig.2. Construction of motion and shape information from these projections is illustrated in Fig.3, and described in the remainder of the Section.

3.1 Motion Information Evaluation.

We split the input video sequence into overlapping temporal blocks. The split allows motion to be captured over a smaller number of frames thus enabling a more detailed analysis of motion. As seen in Fig.3(Set 1), if one motion history template is built for the complete action of 'draw tick', any old motion information gets overwritten when a more recent action occurs at the same point. Not only is part of the motion information lost, but the exact direction of motion (represented by the direction of increasing gray intensity) also gets distorted.

Using overlapping temporal blocks helps to ensure a smooth connectivity of the articulated motion across consecutive blocks. Note that the movement is more continuous in Fig.3(Set 3) as compared to Fig.3(Set 2), in which such a temporal overlap is not maintained.

As mentioned before, the three orthogonal views are handled separately. Firstly, for the complete video sequence we gather all the frame projections for each view. Then, separately for each view,
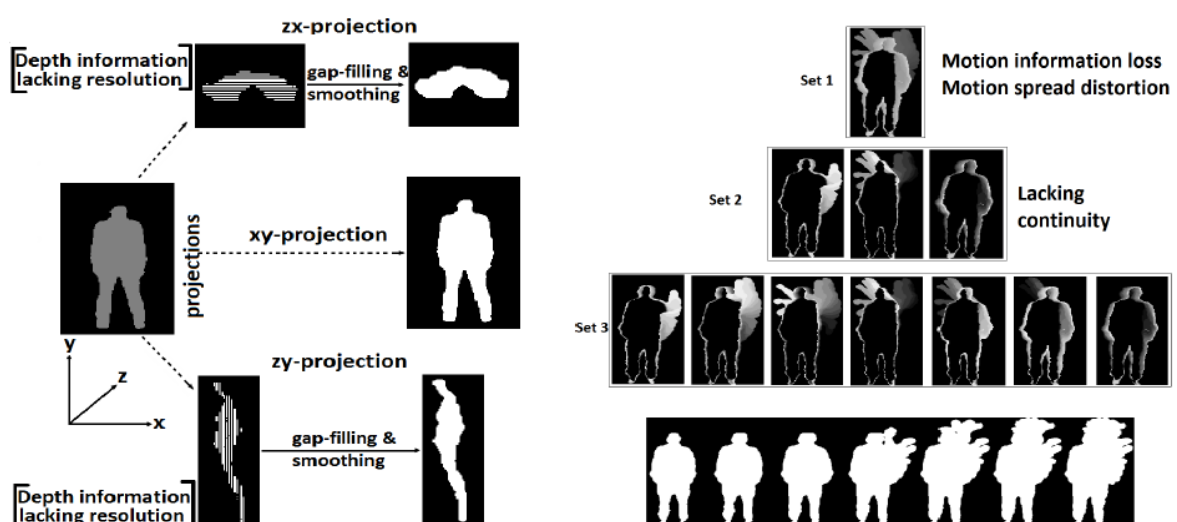

Fig. 2: Depth images projected onto three Cartesian planes to obtain front, side and top views. (Discontinuities resolved using gapfilling and smoothing.)

5

Fig. 3: (Top) Motion history templates for (Set 1) complete sequence, (Set 2) nonoverlapping blocks, (Set 3) overlapping blocks; (Bottom) Binary Shape Templates for a 'draw tick' action focused in the topright region.

we divide the frames into overlapping blocks and proceed to build their motion field. For each block, consecutive frames are subtracted to identify the parts in motion. These parts are stacked together in a weighted manner, with the weight being proportional to the recency of motion, to obtain the desired Motion History Templates.

Namely, the following operations are performed on each block. A motion template MT_f, the difference between two consecutive body silhouettes B_f, is computed as: $MT_f = B_{f+1} - B_f$ for each frame $f \in 1, ..., n - 1$ in the block. The motion history template MHT_b for block b is computed iteratively, by first initializing it to null, and then updating it by applying for each $f \in 1, ..., n-1$ a pixel-wise maximum (p_{max}) of the current motion history template and the weighted motion template $f * MT_f$, namely: $MHT0_b = p_{max}(MHT_b, f * MT_f)$.

3.2. Shape Information Evaluation.

Shape information is constructed in the form of gradient features of binary shape templates, compiled over temporal blocks of the input video sequence. As previously mentioned the three orthogonal views are processed separately. Frame projections for each view are collected and divided into overlapping blocks for which shape templates are constructed. Shape templates become clearer over longer intervals of time and are thus incrementally built, as shown in Fig.3(bottom). The shape template for block 2 is added over the shape template for block 1, the template for block 3 is built over the shape templates for blocks 1 and 2, and so-on.

Thus, the shape template for a given block is built by additive overlaying of body silhouettes, via a frame on frame pixel-wise OR operation, for all the frames in the current as well as the previous blocks. First, the shape template is initialized to $ST_b = ST_{b-1}$, for $b > 1$ (a matrix of zeros otherwise). Then, ST_b is updated iteratively via a pixel-wise OR of the current shape template and the current frame B_f for all frames $f \in 1, ..., n$ as: $ST0_b = ST_b || B_f$.

3.3. Gradient Analysis

Motion history is contained in gray-level variations (MHTs) while shape is represented by white-object boundaries (BSTs). Extraction of shape and motion information therefore necessitates a form of gradient analysis. Herein lies our motivation behind the use of histograms of oriented gradients [24] to obtain the final feature descriptor for the input depth sequence. For the 3D Hand Gesture Dataset, a single histogram of gradients is computed for a complete template, i.e, the standard implementation, where histograms are built over sets of grid cells and later concatenated, is not followed. We observe that different hand gesture enactments have different proportions of gradient values. Thus, without the need for greater discrimination, positions of gradient values could be bypassed. For whole-body datasets, however, the standard HoG implementation is followed. Different regions or body parts can make the same gradient contribution. For examples, actions pairs like - "side boxing and side kick", "forward punch and forward kick", and "high arm wave and two hand wave"; show similar gradient proportions over the complete image but the contributing

gradient regions are different. Thus, for a better discrimination between different action enactments a region-wise gradient analysis is essential.

4. Experimental Settings

4.1. Datasets

We have evaluated the performance of our proposed approach on 4 standard depth datasets - MSR 3D Gesture Dataset [25], MSR 3D Action Dataset [15], 3D Action Pair Dataset [7], and UT-Kinect Database[13]. Details of each database, their preprocessing operations, and the parameter settings for feature extraction are as elaborated below.

MSR 3D Gesture Dataset: The Gesture3D dataset [25] is a hand gesture dataset of depth sequences captured using a depth camera (more particularly a Kinect device). It contains a set of 12 dynamic American Sign Language (ASL) gestures, namely - "bathroom", "blue", "finish", "green", "hungry", "milk", "past", "pig", "store", "where", "j", "z". 10 subjects have performed each hand gesture 2-3 times yielding a total of 336 sample sequences. Sample frames for two gesture categories are shown in Fig.4a. The dataset contains images of hand portions segmented above the wrist and is highly challenging due to self-occlusions in gesture enactments.
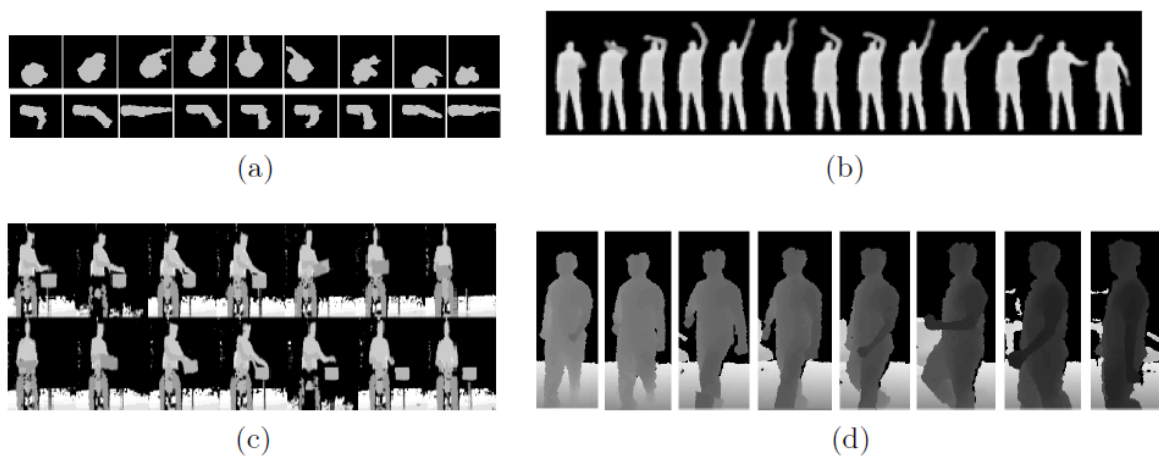

Fig. 4: Sample frames for (a) Hand gesture enactments of 'where', 'pig' (b) Action category of 'high arm wave' (c) Action pairs of 'pick up' & 'put down a box' (d) UT Kinect action category of 'walk'.

MSR 3D Action Dataset: MSR Action3D dataset [15] is an action dataset of depth sequences captured using a depth camera similar to the Kinect device. This dataset contains twenty action categories: "high arm wave", "horizontal arm wave", "hammer", "hand catch", "forward punch", "high throw", "draw x", "draw tick", "draw circle", "hand clap", "two hand wave", "side-boxing", "bend", "forward kick", "side kick", "jogging", "tennis swing", "tennis serve", "golf swing", "pickup & throw". Each action is performed around 2-3 times by 10 subjects, yielding a total of 567 action

samples. Subjects face the camera in the depth maps which are captured at a rate of 15 fps and a resolution of 320Ö 240. Sample frames for a 'high arm wave' action are shown in Fig.4b.

The 20 actions were chosen in the context of using the actions to interact with gaming consoles. They reasonably cover various movements of arms, legs, torso and their combinations. In addition, for actions performed by a single arm or leg, the subjects were advised to use their right arm or leg. In this dataset, the background has been cleaned to remove the discontinuities due to undefined depth points. However, recognition remains highly challenging due to close similarities between different actions.

3D Action Pair Database: This database was introduced by Oreifej and Liu [7] to emphasize the point that two different actions may have similar shape and motion cues, but the correlation between these cues may vary. Quoting the example from [7], "Pick up" and "Put down" actions have similar motion and shape; however, the co-occurrence of object-shape and hand-motion is in different spatio-temporal order and that holds the key to distinguishing the two. Based on this idea, the database puts together 6 action pairs for classification, namely - "Pick up a box/Put down a box", "Lift a box/Place a box", "Push a chair/Pull a chair", "Wear a hat/Take off a hat", "Put on a backpack/Take off a backpack", "Stick a poster/Remove a poster". Each action is performed 3 times using 10 different actors yielding a total of 360 depth sequences. Sample frames presenting an action-pair are as shown in Fig.4c.

UT Kinect Action Database: This database was compiled by Li Xia et al. using a single stationary Kinect camera. It includes 10 action types: "walk", "sitdown", "stand-up", "pick-up", "carry", "throw", "push", "pull", "wave-hands", "clap-hands". Each of the 10 subjects perform each action twice. The UT-Kinect database is highly challenging, with significant variations in single action enactment ('Throw' with left /right arm, 'Carry' with one/both hands, 'walk' - first front-ward and then side-ward as in Fig.4d), action clips duration, frequent occlusions due to changing views, and an annoying shifting background clutter possibly due to camera trembling.

With the frames being recorded only when a skeleton is tracked, the database is biased towards skeleton based processing. The above frame selection also reduces the practical frame rate from 30fps to 15fps. Furthermore, around 2% of the frames have multiple skeletons recorded with slightly different joint locations. Again, using skeleton information the main object can be easily segmented, while in general depth-information processing (as adopted by us) this introduces additional challenges.

4.2. Preprocessing

Images in the hand gesture dataset have varying sizes. For experimental purposes, the images are used as is without any cropping and/or resizing. The aim is to preserve the original shape and gradients in the image. Values in the histograms of gradients are normalized and carry information of the relative gradient proportion. Thus, image size does not affect this normalized distribution.

For the 3 full-body datasets (MSR Action, Action-Pair and UT-Kinect) images need to be uniformly sized to facilitate a more effective grid-based HoG analysis. Also, we can observe that depth information is discontinuous. As can be seen in Fig.2, depth values appear in steps resulting in the black slit-like gaps. The gaps introduce irrelevant gradients. To remove the gaps, we divide each depth value by the average step-size (for gap-filling) and perform small-sized structuring element-based erosion and dilation (for smoothing). This is followed by image packing and resizing (if

required). Finally, the front-view, side-view and top-view templates for the 3 databases are sized: (240x160, 240x180, 180x160); (240x160, 240x480, 480x160); and (320x240, 320x240, 320x320) respectively.

4.3. Parameter settings

To compute our motion analysis descriptors, video sequences (say, of f frames) are divided into t units along the time axis. We move temporally in size of a unit (f /t frames) and in steps decided by the overlap factor (o), to assemble the blocks along the video sequence. Essentially, each block contains f /t frames, and shares 1/o amount of overlap with the previous block. Alternatively, this can be seen as dividing the video into t ∗ o frame sets and grouping o such sets starting at each, to yield a total of: b = (t ∗ o) − (o − 1) blocks.

For each block, motion as well as binary shape templates are constructed for each of the 3 orthogonal views. Thus, for any given video sequence, a maximum of (3*2*b) templates are analyzed. For motion history templates, the direction of motion is stored in grey level variations: hence, all gradients in range 0-360º are considered. For our HoG-based analysis, this range is divided into b1 gradient bins. For shape analysis, a 90º spread was found to be adequate and the 0-90º range is divided into b2 gradient bins. Finally, all the histograms are normalized using the classical L2-norm [24] and concatenated to form the overall feature descriptor.

Dataset specific values for all these parameters are provided below. Presently these are empirically decided, however subsequently we aim to set these parameters via cross validation to boost our performance.

MSR 3D Gesture Dataset: With t = 3 and o = 3, the number of blocks b = 7. We build and analyze a total of 42 (3*2*7) templates to extract motion and shape information. As mentioned previously, for hand gesture templates gradient analysis is done once for the complete image without any division into smaller grids. b1 and b2 are set to 72 and 18 respectively.

MSR 3D Action Dataset: With t = 3 and o = 3, the number of blocks b = 7. We build and analyze a total of 42 (3*2*7) templates. The 7 motion history templates and 7 shape templates for front-view of 'draw tick' action are as shown in Fig.3 (Set 3) & (bottom). Further, for HoG analysis, the front, side and top views of motion history templates are divided into 6x4, 6x4 and 4x4 non-overlapping grid blocks while for shape templates they are divided into 1x1, 1x1 and 1x1 sized grid blocks. b1 and b2 are set to 36 and 9 respectively.

3D Action Pair Database: With t = 4 and o = 2, the number of blocks b = 7. We build and analyze a total of 42 (3*2*7) templates. For HoG analysis, front, side and top views of motion history templates are divided into 6x4, 6x8 and 8x4 non-overlapping grid blocks while for shape templates they are divided into 1x1, 1x1 and 1x1 sized grid blocks. b1 and b2 are set to 36 and 9 respectively.

UT Kinect Action Database: With t = 4 and o = 2, the number of blocks b = 7. We build and analyze a total of 21 (3*1*7) templates. Due to significant variations in view and action enactment, as well frequent occlusions and camera motion, we observed shape templates to be counter-productive and hence shape templates were not considered. For HoG analysis, front, side and top views of motion history templates are divided into 3x4, 3x4 and 4x4 non-overlapping grid blocks. In place of shape templates, motion history templates are additionally analyzed over 1x1, 1x1 and 1x1 sized grid blocks. b1 is set to 36.

Approach	Accuracy (%)
Proposed (MHI + BST based Gradient Analysis)	96.6
Oreifej & Liu[7]	92.45
Jiang et al.[17]	88.5
Kurakin et al.[25]	87.77

Fig. 5: Accuracy comparison for 3D Hand Gesture Recognition.

	z	j	where	store	pig	past	hungry	green	finish	blue	bathroom	milk
z	100	0	0	0	0	0	0	0	0	0	0	0
j	0	100	0	0	0	0	0	0	0	0	0	0
where	0	0	93.3	0	0	0	0	0	6.66	0	0	0
store	0	0	0	93.3	0	0	0	0	0	6.66	0	0
pig	0	0	0	0	100	0	0	0	0	0	0	0
past	0	0	0	0	0	100	0	0	0	0	0	0
hungry	0	0	0	0	0	0	100	0	0	0	0	0
green	0	0	0	0	0	0	0	100	0	0	0	0
finish	0	0	0	0	0	0	0	0	100	0	0	0
blue	0	0	0	6.66	0	0	0	0	0	100	0	0
bathroom	0	0	0	0	0	0	0	0	0	0	100	0
milk	0	0	0	0	0	0	0	6.66	0	0	0	93.3

Fig. 6: Confusion matrix for 3D hand gesture recognition using the proposed approach.

5. Recognition Results

We use SVM [26] discriminative classifier in one-versus-one configuration for the task of multi-class classification. In order to handle non-linear class boundaries SVM uses radial basis function kernel.

MSR 3D Gesture Dataset: As per the standard protocol, for every gesture category samples of first 5 subjects form the training set while those of next 5 subjects form the test set. With this cross-subject

accuracy of 96.6% our proposed method significantly outperforms the existing best [7]. Fig.5 lists the comparison with the previously attempted approaches for the given dataset. The related confusion matrix is presented in Fig.6.

MSR 3D Action Dataset: Our approach yields a cross-subject accuracy of 83.8%. Fig.7 presents the performance comparison with previously attempted approaches for the given dataset. Related confusion matrix is presented in Fig.8. Jiang et al. [8] obtain an accuracy figure of 88.20% with skeleton tracking approach. However, it has the drawback of being dependent on the precision of 3D joints positions making it susceptible to occlusion errors. Yang et al. [21], Vieira et al.[16], Li et al. [15] perform experiments on three subsets of the 3D Action dataset – AS1, AS2 and AS3, containing 8 action categories each. Confusion among a set of categories is always greater than or equal to the confusion in its subsets. Hence, the correct overall-accuracy for the approaches is not the average of the 3 subset accuracies but lesser than the minimum amongst the 3 values i.e. < 84.1%, < 81.30% and < 71.90% respectively. Considering the HoN4D approach on equal grounds i.e. without data-specific quantization refining [7], the accuracy of our approach is 2% lower.

Given the performance of our approach on the other 3 datasets, we can argue that the relatively low accuracy is mainly due to inadequate data. The number of classes is the highest (20), but the number of sample videos per class is the same as in other datasets. We believe that with a higher number of videos our approach would generalize better to test set.

Approach	Accuracy (%)
Proposed (MHI + BST based Gradient Analysis)	83.8
Oreifej & Liu [7]	88.89
Jiang et al. [8]	88.2
Jiang et al. [17]	86.5
Yang et al. [21]/ [7]	<84.1/ 85.52
Vieira et al.[16]	<81.30
Li et al. [15]	<71.90

Fig. 7: Accuracy comparison for 3D Action Data Recognition.

	high arm wave	horizontal arm wave	hammer	hand catch	forward punch	high throw	draw x	draw tick	draw circle	hand clap	two hand wave	side boxing	bend	forward kick	side kick	jogging	tennis swing	tennis serve	golf swing	pick up & throw
high arm wave	100	0	0	0	0	0	0	0	0	0	0	0	0	0	0	0	0	0	0	0
horizontal arm wave	0	100	0	0	0	0	0	0	0	0	0	0	0	0	0	0	0	0	0	0
hammer	0	0	0	0	26.7	0	20	0	53.3	0	0	0	0	0	0	0	0	0	0	0
hand catch	0	0	0	66.7	0	0	6.66	6.66	6.66	0	0	13.3	0	0	0	0	0	0	0	0
forward punch	0	0	0	0	92.9	7.14	0	0	0	0	0	0	0	0	0	0	0	0	0	0
high throw	21.4	0	0	14.3	0	64.3	0	0	0	0	0	0	0	0	0	0	0	0	0	0
draw x	0	14.3	0	0	0	0	50	0	35.7	0	0	0	0	0	0	0	0	0	0	0
draw tick	0	0	0	6.66	0	0	0	93.3	0	0	0	0	0	0	0	0	0	0	0	0
draw circle	6.66	0	0	0	0	0	6.66	0	86.7	0	0	0	0	0	0	0	0	0	0	0
hand clap	0	0	0	0	0	0	0	0	0	100	0	0	0	0	0	0	0	0	0	0
two hand wave	0	0	0	0	0	0	0	0	0	0	100	0	0	0	0	0	0	0	0	0
side boxing	0	0	0	0	0	0	0	0	0	0	0	100	0	0	0	0	0	0	0	0
bend	0	0	0	0	0	0	0	0	0	0	0	0	93.3	6.66	0	0	0	0	0	0
forward kick	0	0	0	0	0	0	0	0	0	0	0	0	0	100	0	0	0	0	0	0
side kick	0	0	0	0	0	0	0	0	0	0	0	6.66	0	0	73.3	0	0	6.66	13.3	0
jogging	0	0	0	0	0	0	0	0	0	0	0	0	0	0	0	93.3	0	6.66	0	0
tennis swing	0	0	0	0	0	0	0	0	0	0	0	0	0	0	0	0	100	0	0	0
tennis serve	0	0	0	0	0	0	0	0	0	0	0	0	0	0	0	0	20	80	0	0
golf swing	0	0	0	0	0	0	0	0	0	0	0	0	0	0	0	0	0	0	100	0
pick up & throw	0	0	0	6.66	0	0	0	0	0	0	0	0	6.66	0	0	0	0	0	0	86.7

Fig. 8: Confusion matrix for 3D action data recognition using the proposed approach.

3D Action Pair Database: A cross-subject accuracy of 97.22% indicates that if sufficient amount of data is available per action category, our proposed approach has the potential to give top recognition results. Fig.9 presents the performance comparison with other approaches. The related confusion matrix is shown in Fig.10.

UT Kinect Action Database: To the best of our knowledge, our approach is the only non-skeleton based technique attempted for UT Kinect Database. Despite the data being biased for skeletal analysis, as explained in Section 4.1, our method gives a competitive accuracy of 90% (under the same testing conditions as in [13]) compared to the authors' 90.92%.

Approach	Accuracy (%)
Proposed (MHI + BST based Gradient Analysis)	97.22
Oreifej & Liu [7]	96.67
Jiang et al. [8]	82.22
Yang et al. [21]	66.11

Fig. 9: Accuracy comparison for 3D action-pair data recognition.

	Pick up a box	Put down a box	Lift a box	Place a box	Push a chair	Pull a chair	Wear a hat	Take off a hat	Put on a backpack	Take off a backpack	Stick a poster	Remove a poster
Pick up a box	100	0	0	0	0	0	0	0	0	0	0	0
Put down a box	0	100	0	0	0	0	0	0	0	0	0	0
Lift a box	0	0	93.3	6.66	0	0	0	0	0	0	0	0
Place a box	0	0	0	100	0	0	0	0	0	0	0	0
Push a chair	0	0	0	0	100	0	0	0	0	0	0	0
Pull a chair	0	0	0	0	0	100	0	0	0	0	0	0
Wear a hat	0	0	0	0	0	0	100	0	0	0	0	0
Take off a hat	0	0	0	0	0	0	6.66	93.3	0	0	0	0
Take off a backpack	0	0	0	0	0	0	0	0	100	0	0	0
Stick a poster	0	0	0	0	0	0	0	0	0	100	0	0
Remove a poster	0	0	0	0	0	0	0	0	0	0	100	0
Put on a backpack	0	13.3	0	0	0	0	0	0	0	0	0	86.7

Fig. 10: Confusion matrix for 3D action-pair data recognition using the proposed approach.

6. Performance under Occlusion and Noise

The performance of the proposed approach has also been evaluated in the presence of two noise effects as elaborated in the subsections below. Results have been compiled on MSR 3D Action Database. 6.1 Occlusion To analyze and compare the robustness of our method in the presence of occlusion, we carried out an experiment similar to that presented in [15]. As shown in Fig.11, for a given occlusion setting, a single quadrant or a combination of 2 quadrants may be occluded in the

depth image. Occlusion is incorporated in the test set and Fig.12 shows the relative accuracy for each case. (Relative accuracy is defined as the recognition accuracy with occlusion, as a percentage of the accuracy without any occlusion).
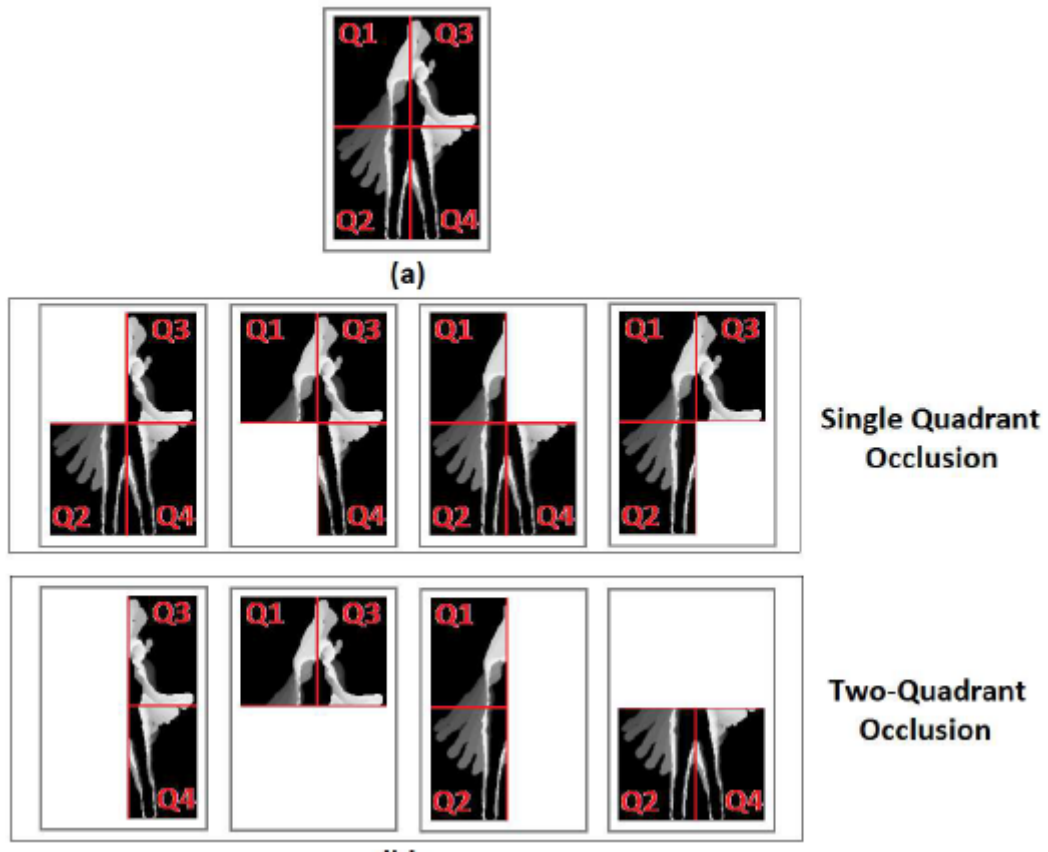

Fig. 11: Occlusion of quadrant(s) for robustness testing.

With most of the actions focused on the top-right of the image, occlusion of Q3 gives the highest error rate. For all other single quadrant occlusions, accuracy reduction is no greater than 9%. Our method has the potential to handle occlusions primarily because it performs an independent region-wise gradient analysis over motion history and shape templates. Even if a particular part of the image is occluded, visible body regions are unaffected and can be independently analyzed.

Occluded Quadrant(s)	Relative Accuracy (%)
none	100
Q1	91.57
Q2	95.99
Q3	64.66
Q4	96.39
Q1+Q3	43.376
Q3+Q4	62.25
Q4+Q2	85.948
Q2+Q1	65.87

Fig. 12: Recognition performance of the proposed approach in presence of occlusion.

6.2. Pepper Noise

The most common error that affects depth images, and consequently renders interest point approaches ineffective, is the presence of discontinuous black regions in the images. In a completely new performance measure, we deliberately introduce pepper noise in different percentages (of the total number of image pixels) in the depth images, as in Fig.13. From Fig.14, the recognition accuracy does not fall by more than 6% even in up to 10% pepper noise. This indicates the high robustness of our method to depth discontinuities.
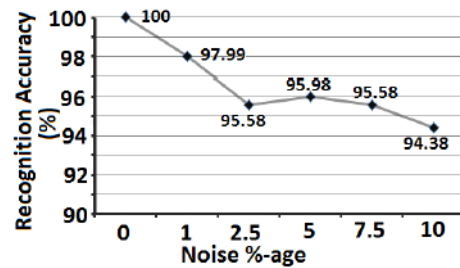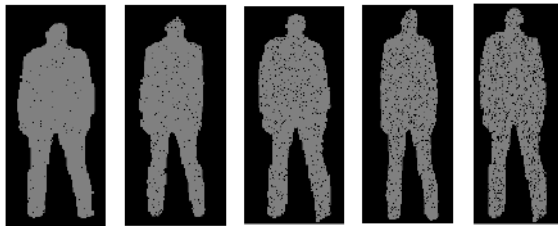

Fig. 13: Images affected by pepper noise in increasing percentages of total no. of pixels - 1%, 2.5%, 5%, 7.5% and 10%.

Fig. 14: Recognition performance of the proposed approach in presence of varying amount of pepper noise (to simulate depth discontinuities).

7. Conclusion and Future Work

This paper presents a compact and inexpensive global descriptor for activity recognition from depth videos. The overall approach performs consistently well on 4 very different databases. It outperforms the existing best on 2 out of 3 standard depth databases and is the first non-skeleton based approach to give highly competitive results on UT Kinect Action Database. This proves its generic performance and wide applicability. Also, experimental results confirm its ability to handle occlusion and noise errors that commonly affect depth images. As part of the future work, we will set the parameters of block-size (1/t) and overlap-factor (o) via cross-validation to achieve improved performance through a database-specific setting. Also, we aim to assess the applicability of our approach to real-time action recognition from online depth videos. Temporal blocks can be treated as independent observation states. A model can be made to learn the observation-state-transition-probability to action-category mapping. Thus, temporal blocks and their sequence can help identify the action enacted in a live video. With every incoming block, the decision needs to be reconsidered in the light of the most recent input information.

References

1. Laptev, I., Lindeberg, T.: Space-time interest points. In: ICCV, IEEE Computer Society (2003) 432–439.
2. Dollar, P., Rabaud, V., Cottrell, G., Belongie, S.: Behavior recognition via sparse spatio-temporal features. In: Proceedings of the 14th International Conference on Computer Communications and Networks. ICCCN '05, Washington, DC, USA, IEEE Computer Society (2005) 65–72.
3. Klaser, A., Marszalek, M., Schmid, C.: A spatio-temporal descriptor based on 3d-gradients. In Everingham, M., Needham, C.J., Fraile, R., eds.: BMVC, British Machine Vision Association (2008).
4. Yilmaz, A., Shah, M.: Actions sketch: A novel action representation. In: CVPR (1), IEEE Computer Society (2005) 984–989.
5. Gorelick, L., Blank, M., Shechtman, E., Irani, M., Basri, R.: Actions as space-time shapes. IEEE Trans. Pattern Anal. Mach. Intell. 29 (2007) 2247–2253.
6. Li, W., Zhang, Z., Liu, Z.: Expandable data-driven graphical modeling of human actions based on salient postures. IEEE Trans. Circuits Syst. Video Techn. 18 (2008) 1499–1510.
7. Oreifej, O., Liu, Z.: Hon4d: Histogram of oriented 4d normals for activity recognition from depth sequences. In: Computer Vision and Pattern Recognition (CVPR), 2013 IEEE Conference on. (2013) 716–723.
8. Wang, J., Liu, Z., Wu, Y., Yuan, J.: Mining actionlet ensemble for action recognition with depth cameras. In: Computer Vision and Pattern Recognition (CVPR), 2012 IEEE Conference on. (2012) 1290–1297.
9. Shotton, J., Fitzgibbon, A., Cook, M., Sharp, T., Finocchio, M., Moore, R., Kipman, A., Blake, A.: Real-time human pose recognition in parts from single depth images. In: Computer Vision and Pattern Recognition (CVPR), 2011 IEEE Conference on. (2011) 1297–1304.
10. Yun, H., Sheng-Luen, C., Jeng-Sheng, Y., Qi-Jun, C.: Real-time skeleton-based indoor activity recognition. In: Control Conference (CCC), 2013 32nd Chinese. (2013) 3965–3970.
11. Shuzi, H., Jing, Y., Huan, C.: Human actions segmentation and matching based on 3d skeleton model. In: Control Conference (CCC), 2013 32nd Chinese. (2013) 5877–5882.

12. Yu, X., Wu, L., Liu, Q., Zhou, H.: Children tantrum behaviour analysis based on kinect sensor. In: Intelligent Visual Surveillance (IVS), 2011 Third Chinese Conference on. (2011) 49–52.

13. Xia, L., Chen, C.C., Aggarwal, J.: View invariant human action recognition using histograms of 3d joints. In: Computer Vision and Pattern Recognition Workshops (CVPRW), 2012 IEEE Computer Society Conference on. (2012) 20–27.

14. : (Efficient model-based 3d tracking of hand articulations using kinect).

15. Li, W., Zhang, Z., Liu, Z.: Action recognition based on a bag of 3d points. In: Computer Vision and Pattern Recognition Workshops (CVPRW), 2010 IEEE Computer Society Conference on. (2010) 9–14.

16. Vieira, A., Nascimento, E., Oliveira, G., Liu, Z., Campos, M.: Stop: Space-time occupancy patterns for 3d action recognition from depth map sequences. In Alvarez, L., Mejail, M., Gomez, L., Jacobo, J., eds.: Progress in Pattern Recognition, Image Analysis, Computer Vision, and Applications. Volume 7441 of Lecture Notes in Computer Science. Springer Berlin Heidelberg (2012) 252–259.

17. Wang, J., Liu, Z., Chorowski, J., Chen, Z., Wu, Y.: Robust 3d action recognition with random occupancy patterns. In: Proceedings of the 12th European Conference on Computer Vision - Volume Part II. ECCV'12, Berlin, Heidelberg, SpringerVerlag (2012) 872–885.

18. Bobick, A.F., Davis, J.W.: The recognition of human movement using temporal templates. IEEE Trans. Pattern Anal. Mach. Intell. 23 (2001) 257–267.

19. Davis, J.W.: Hierarchical motion history images for recognizing human motion. In: IEEE Workshop on Detection and Recognition of Events in Video. (2001) 39–46.

20. Tian, Y., Cao, L., Liu, Z., Zhang, Z.: Hierarchical filtered motion for action recognition in crowded videos. Systems, Man, and Cybernetics, Part C: Applications and Reviews, IEEE Transactions on 42 (2012) 313–323.

21. Yang, X., Zhang, C., Tian, Y.: Recognizing actions using depth motion maps-based histograms of oriented gradients. In: Proceedings of the 20th ACM International Conference on Multimedia. MM '12, New York, NY, USA, ACM (2012) 1057–1060.

22. Megavannan, V., Agarwal, B., Venkatesh Babu, R.: Human action recognition using depth maps. In: Signal Processing and Communications (SPCOM), 2012 International Conference on. (2012) 1-5.

23. Weinland, D., Ronfard, R., Boyer, E.: Free viewpoint action recognition using motion history volumes. Comput. Vis. Image Underst. 104 (2006) 249–257.

24. Dalal, N., Triggs, B.: Histograms of oriented gradients for human detection. In: Computer Vision and Pattern Recognition, 2005. CVPR 2005. IEEE Computer Society Conference on. Volume 1. (2005) 886–893 vol. 1.

25. Kurakin, A., Zhang, Z., Liu, Z.: A real time system for dynamic hand gesture recognition with a depth sensor. In: Signal Processing Conference (EUSIPCO), 2012 Proceedings of the 20th European. (2012) 1975–1979.

26. Chang, C.C., Lin, C.J.: Libsvm: A library for support vector machines. ACM Trans. Intell. Syst. Technol. 2 (2011) 27:1–27:27